



Published in final edited form as:

Biol Psychiatry. 2009 June 1; 65(11): 943–950. doi:10.1016/j.biopsych.2008.10.007.

Preclinical Atherosclerosis Covaries with Individual Differences in Reactivity and Functional Connectivity of the Amygdala

Peter J. Gianaros, Ahmad R. Hariri, Lei K. Sheu, Matthew F. Muldoon, Kim Sutton-Tyrrell, and Stephen B. Manuck

Departments of Psychiatry and Psychology (PJM, ARH), Department of Psychiatry (LKS), Department of Medicine (MFM), Department of Epidemiology (KS-T), and Department of Psychology (SBM), University of Pittsburgh, Pittsburgh, Pennsylvania

Abstract

Background—Cardiovascular disease (CVD) is a major source of medical comorbidity for patients with mood and anxiety disorders, and it remains the leading public health burden for the general population in industrialized nations. Indirect neurobiological evidence suggests that preclinical risk for atherosclerosis, the main contributor to CVD, may be conferred by interindividual variation in the functionality of the amygdala, a brain system jointly involved in processing behaviorally salient stimuli and regulating the cardiovascular system.

Methods—In a neuroimaging study of 36 middle-aged adults (18 women) who were screened for confounding clinical cardiovascular and psychiatric disorders, we examined the direct covariation between a marker of preclinical atherosclerosis, carotid artery intima-media thickness (IMT), and interindividual variation in amygdala reactivity and functional connectivity assessed during the processing of behaviorally salient stimuli (angry and fearful facial expressions).

Results—After accounting for traditional CVD risk factors, a thickening of carotid IMT across individuals covaried with greater amygdala reactivity and a more positive functional connectivity between the amygdala and perigenual anterior cingulate cortex, a corticolimbic area also implicated in behavioral salience processing and cardiovascular regulation.

Conclusions—Individual differences in amygdala reactivity and functional connectivity may reflect facets of a novel, systems-level neural phenotype conferring risk for atherosclerosis and CVD.

Keywords

Amygdala; anterior cingulate cortex; cardiovascular disease risk; carotid intima-media thickness; preclinical atherosclerosis

Cardiovascular disease (CVD) remains the leading cause of premature death and disability in industrialized nations (1). Cardiovascular disease also shows appreciable comorbidity with mood and anxiety disorders characterized by dysregulated cardiovascular function (2-5). The clinical end points of CVD, including angina, myocardial infarction, and stroke, result primarily from atherosclerosis, an inflammatory syndrome affecting the lining of major arteries (6). Beginning early in life, atherosclerosis progresses from clinically silent or preclinical changes in arterial morphology to the emergence of obstructive plaques that precipitate CVD

end points later in life (7). Over the life span, however, the progression and severity of atherosclerosis vary across individuals as a function of biological and behavioral risk factors.

At the epidemiologic level, for example, risk for atherosclerosis has long been associated with individual differences in sensitivity and reactivity to behaviorally salient stimuli, including stimuli that are biologically relevant, emotionally evocative, or that engage evaluative processes supporting behavioral action (e.g., fight-or-flight) (8). This biobehavioral dimension of atherosclerotic risk is presumably conferred by interindividual variation in co-occurring adjustments in autonomic and neuroendocrine outflow to the cardiovascular system, as indicated by human (9-12) and nonhuman primate (13-15) studies. Critically, while such physiological adjustments may support adaptive behavioral action, they may also accelerate atherosclerotic progression by facilitating proinflammatory and preclinical arterial changes among vulnerable individuals (8,16). At the neural level, these potentially atherogenic physiological adjustments are likely orchestrated by brain circuitries that jointly 1) assign behavioral salience to environmental stimuli and 2) regulate cardiovascular function via projections to preautonomic and neuroendocrine control areas (16). More precisely, recent evidence suggests that circuitries networked with the amygdala may regulate peripheral cardiovascular mechanisms implicated in atherogenesis (17).

Within a complex intra-amygdala circuitry, the central nucleus of the dorsal amygdala specifically regulates the effector arms of the autonomic nervous system and hypothalamic-pituitary-adrenal axis by signaling with corticolimbic, diencephalic, and mesencephalic areas involved in cardiovascular control (18,19). By this circuitry, individual differences in amygdala functionality may thus relate to autonomic, cardiovascular, and neuroendocrine processes promoting atherosclerotic risk. Consistent with this notion, recent neuroimaging evidence demonstrates that individual differences in amygdala reactivity to behaviorally salient stimuli covary with physiological parameters associated with preclinical atherosclerosis, including basal levels of autonomic cardiac control (20), stressor-evoked changes in blood pressure (17), and diurnal variation in the secretion of the stress hormone, cortisol (21). Nevertheless, it remains unknown whether individual differences in amygdala reactivity and functionality per se covary directly with a marker of preclinical atherosclerosis, thus implicating the amygdala in mediating atherogenic changes preceding late-stage CVD end points.

Accordingly, we tested whether carotid artery intima-media thickness (IMT), a marker of preclinical atherosclerosis predictive of incident CVD end points (22-26), would covary with individual differences in amygdala reactivity to behaviorally salient stimuli (angry and fearful facial expressions) in adults free of psychiatric and cardiovascular disorders. Next, we tested whether carotid IMT would covary with the correlated activity (functional connectivity) between the amygdala and anterior cingulate cortex (ACC). The ACC is a corticolimbic area networked with the amygdala (27-29) that has been implicated by recent work to functionally interact with the amygdala in the prediction of individual differences in cardiovascular responses implicated in atherogenesis (17). Finally, we explored whether any covariation between carotid IMT and amygdala reactivity or connectivity could be explained by interindividual variation in traditional CVD risk factors.

Methods and Materials

Participants

Participants were 36 adults (aged 31–53, half women) recruited from a previously described (20,30) epidemiological study, the Adult Health and Behavior Project (AHAB). The Adult Health and Behavior Project is a community-based registry of 1379 adults from Southwestern Pennsylvania who have been characterized for CVD risk factor covariation. Exclusion criteria included any DSM-IV Axis I psychiatric disorder determined by structured clinical interview

(31), any cardiovascular or cerebrovascular disease, any chronic health condition, and any medication regimen that could confound study findings. Supplement 1 provides additional recruitment, screening, and participant details. All participants consented to study protocols, approved by The University of Pittsburgh Institutional Review Board.

CVD Risk Factor Assessment

Cardiovascular disease risk factors were assessed during a clinic visit between 7:30 AM to 10:30 AM, after a 12-hour fast. Seated resting blood pressure, body mass index, and serum lipids, glucose, and insulin levels were assessed by methods detailed previously (32). Education and annual income were assessed by self-report (see Table 1 for coding). Depressive symptoms and dispositional anxiety, previously associated with preclinical atherosclerosis in some epidemiological studies (33), were assessed by the Center for Epidemiological Studies Depression Scale (CES-D) (34) and the Trait scale of the Spielberger State-Trait Anxiety Inventory (STAI-T) (35). CES-D and STAI-T scores did not approach cutoffs suggesting clinical depression or anxiety in this sample; also, neither CES-D nor STAI-T scores correlated significantly with IMT (Table 1).

Carotid IMT Assessment

The mean IMT of the carotid vessel wall complex (in mm) was assessed by B-mode ultrasonography (36,37). Carotid IMT is used as a marker of preclinical atherosclerosis in epidemiological studies (26) and as a surrogate measure of coronary atherosclerosis in clinical trials (22,24,25). For ultrasonography, a vascular technologist using an Acuson Antares scanner (Acuson-Siemens, Malvern, Pennsylvania) first obtained scout images of the left and right carotid arteries while the participant was supine (head tilted by $\approx 45^\circ$). After scout imaging, a region of interest (ROI) encompassing the artery walls was identified for focused imaging of three segments: 1) the near and far walls of the distal common carotid (1 cm proximal to the carotid bulb); 2) the far wall of the carotid bulb (defined as the point where the near and far walls of the common carotid diverge, extending to the flow divider); and 3) the far wall of the first centimeter of the internal carotid (defined distally from the point of the flow divider). For these segments, an image was digitized for quantitative scoring by automated edge detection software (Artery Measurement System; Goteborg University, Gothenburg, Sweden) (38). The software defined two digital lines to quantify IMT, one along the lumen-intima interface and one along the media-adventitia interface. The distances between these two lines were measured over 1 cm for each segment (with the exception of the bulb, measured in its entirety), generating one IMT measurement (in mm) per pixel in each segment (≈ 140 measurements per segment) (Figure 1).

For all segments, average IMT measurements were recorded, and mean IMT was computed as the grand average of all measurements from the right and left carotid arteries. In addition to mean IMT, we assessed the frequency of carotid plaques, defined as focal protrusions where IMT was at least 50% greater than adjacent areas. Only four individuals had detectable plaques. Hence, plaque frequency was not evaluated in association with neuroimaging measures. Importantly, study results were unchanged in direction and statistical significance when these four individuals were omitted from all analyses.

Amygdala Reactivity Protocol

To elicit amygdala reactivity during one functional magnetic resonance imaging (fMRI) run of 390 sec, participants completed a standardized protocol comprised of four blocks of a facial expression matching task interleaved with five blocks of a shape-matching control task. This protocol, detailed previously (39-41), evokes reliable individual differences in amygdala reactivity. In two blocks of angry and two blocks of fearful facial expression matching trials, participants viewed an array of three faces per trial (all of one target expression) and selected

via button press on a fiber optic response glove one of two (at bottom) that matched a center target (at top). Each facial expression matching block consisted of six trials (4 sec presentation times; variable 2–6 sec intertrial interval; three trials of each gender). All expressions were from a standard stimulus set (42). In five blocks of shape-matching control trials, participants viewed three shapes (vertical and horizontal ellipses and circles) and selected one of two (at bottom) that matched a center target (at top). Each shape-matching block consisted of six trials presented sequentially for 4 sec. All blocks were preceded by an instruction: “Match Faces” or “Match Shapes.” Across individuals, face- and shape-matching accuracy exceeded 99%.

Neuroimaging Data Acquisition

Neuroimaging data were acquired on a 3T MAGNETOM Allegra head-dedicated scanner (Siemens, Erlangen, Germany). For spatial normalization of blood oxygenation level-dependent (BOLD) images, T2-weighted structural images were acquired prior to the amygdala reactivity protocol (repetition time [TR]/echo time [TE] 6530/95 msec; flip angle 150°; 34 axial-oblique slices; field of view [FOV] 200 mm; in-plane resolution .8 × .8 mm; slice thickness 3 mm [no gap]). BOLD images were acquired during the reactivity protocol with a gradient-echo echo planar imaging (EPI) sequence encompassing the entire cerebrum and majority of the cerebellum (TR/TE 2000/25 msec; flip angle 70°; 34 axial-oblique slices; FOV 200 mm; in-plane resolution 3.125 × 3.125 mm; slice thickness 3 mm [no gap]; four initial discarded volumes). BOLD image quality was enhanced through fast gradients (slew rate 400 T/m/s), which minimized echo-spacing and reduced EPI geometric distortion. Before data acquisition, a reference BOLD image was obtained and inspected for artifacts (e.g., ghosting), ensuring signal quality across the acquisition volume, particularly in slices encompassing the amygdala.

Neuroimaging Data Preprocessing

Neuroimaging data were preprocessed and analyzed with statistical parametric mapping software (SPM5; <http://www.fil.ion.ucl.ac.uk/spm>, Wellcome Trust Centre for Neuroimaging, London, United Kingdom). For preprocessing, BOLD images were realigned to the first image of the series, co-registered to T2-weighted structural images, normalized to the International Consortium for Brain Mapping 152 template (Montreal Neurological Institute [MNI]), and smoothed with an 8 mm isotropic Gaussian kernel.

Analysis of Carotid IMT and Amygdala Reactivity

After preprocessing, a contrast image reflecting BOLD reactivity (faces > shapes activation) was estimated for each individual. For this purpose, face- and shape-matching blocks were modeled with rectangular waveforms convolved with the default statistical parametric mapping hemodynamic response function; contrast images were then generated by general linear model (GLM) estimation. Prior to estimation, low-frequency BOLD signal drift was removed by high-pass filtering (128 sec cutoff); serial BOLD signal autocorrelations were also corrected with a first-order autoregressive model.

To determine the covariation between carotid IMT and BOLD reactivity at the group level, individual contrast images were submitted to a regression model in SPM5. In the model, carotid IMT was entered as a regressor of interest, with age, sex, resting systolic blood pressure (SBP), and family income entered as covariates. These covariates were selected because they were associated with carotid IMT at $p < .05$ (Table 1). Following study hypotheses, the covariation between carotid IMT and amygdala reactivity across individuals was tested using anatomical ROI masks described next.

Amygdala ROI Analyses

Areas of the amygdala are partitioned by histological criteria, trajectories of efferent and afferent fibers, and corresponding functional processes (18,43-46). The dorsal amygdala, encompassing the central nucleus, has reciprocal connections with corticolimbic, diencephalic, and mesencephalic areas involved in cardiovascular regulation (9-12,14,16). The ventral amygdala, encompassing the basolateral area, is understood to integrate polymodal sensory inputs from association areas to support stimulus encoding and memory processes (9-12,14, 16). Given the role of the dorsal amygdala in regulating cardiovascular processes pertinent to atherosclerotic risk, we tested whether carotid IMT would covary with reactivity of the dorsal, but perhaps not ventral, amygdala. For this test, we constructed dorsal and ventral amygdala ROIs prior to data analysis (Supplement 2). For all amygdala ROI analyses, we applied a corrected false discovery rate (FDR) threshold (47) of $p < .05$ and voxel extent threshold of $k = 20$.

Analysis of Carotid IMT and Amygdala-ACC Connectivity

In separate functional connectivity analyses, we tested whether carotid IMT covaried with the direction and strength of temporally correlated BOLD signal changes between the amygdala and ACC. For these analyses, we extracted the mean BOLD signal time series from the right and left amygdala for each individual using MarsBar (48). Specifically, a time series was extracted from the mean BOLD signal of all voxels within a 5 mm sphere surrounding the amygdala coordinates identified in the regression analyses of carotid IMT and dorsal amygdala reactivity reported below (left amygdala x, y, z MNI seed: -16, -8, -14; right amygdala seed: 20, -6, -14). Extracted time series were mean-centered, drift-corrected, and inspected for outliers. Any outlying values >3 SD of the series mean were replaced by the average of two surrounding values. The outlier-corrected time series were then entered as regressors in individual GLM SPM5 design matrices. Also, given that functional connectivity analyses are prone to confounding by cardiac, respiratory, and other nonspecific sources of noise, we extracted a cerebrospinal fluid (CSF) time series from the fourth ventricle (0, -43, -26) and included this series as a nuisance regressor in individual GLM matrices. Finally, for all individual-level connectivity analyses, low-frequency BOLD signal drift was high-pass filtered (128 sec cutoff), and high-frequency BOLD signal autocorrelations were corrected with a first-order autoregressive model. For each individual, this routine yielded a functional connectivity map identifying areas where BOLD signal changes cross-correlated with signal changes in the amygdala seeds.

To determine the covariation between carotid IMT and amygdala-ACC functional connectivity across individuals, individual connectivity maps were submitted to a regression model in SPM5. In the model, carotid IMT was entered as a regressor of interest, with age, sex, resting SBP, and family income entered as covariates as in the reactivity analyses described above. The covariation between carotid IMT and amygdala-ACC functional connectivity across individuals was tested using an anatomical mask of the ACC described in Supplement 2. For the ACC ROI analysis, we applied a corrected threshold of $p_{\text{FDR}} < .05$ and extent threshold of $k = 20$. We emphasize that the connectivity values reported herein do not reflect inhibitory, excitatory, or causal (effective) associations between amygdala and ACC activity (49).

Whole-Brain and Supplementary Analyses

For exploratory purposes, we executed regression analyses testing for covariation between carotid IMT and 1) whole-brain BOLD reactivity (faces $>$ shapes activation) and 2) amygdala functional connectivity in SPM5. For BOLD reactivity analyses, we generated a parametric map identifying all areas engaged by the facial expression matching task (revealed by the faces $>$ shapes contrast) in a mixed-effects model executed with a threshold of $p_{\text{FDR}} = .05$, $k = 20$. In a regression analysis with inclusive masking, we then tested for covariation between carotid

IMT and activation in areas revealed by this whole-brain analysis at a lenient threshold of $p_{\text{uncorrected}} < .001$, $k = 20$. For exploratory functional connectivity analyses, we tested for covariation between carotid IMT and connectivity with the left and right amygdala seeds described above in an unmasked whole-brain regression model, also executed at $p_{\text{uncorrected}} < .001$, $k = 20$. In all regressions, age, sex, resting SBP, and income were entered as covariates.

Supplementary analyses were also executed outside of SPM5 to explore whether carotid IMT covaried uniquely with extracted amygdala BOLD reactivity values (faces > shapes contrast parameters) and extracted amygdala-ACC connectivity values (plotted in Figures 2 and 3). Here, we used two-step hierarchical regression models in SPSS software (v16, SPSS Inc., Chicago, Illinois) to partition the variance in carotid IMT accounted for by reactivity and connectivity values (entered in step 2 of the models), over and above the covariates used in SPM5 analyses (sex, age, resting SBP, income), as well as other traditional CVD risk factors derived from serum assays that correlated with carotid IMT at r 's $\geq .20$; namely, total cholesterol, low-density lipoprotein (LDL), and triglyceride concentrations (Table 1). In the models, the test statistic was the ΔR^2 from step 1 to step 2.

Results

Carotid IMT and Amygdala Reactivity

Carotid IMT covaried positively across individuals with dorsal amygdala reactivity to angry and fearful facial expressions (Figure 2). Notably, this finding was obtained with covariate control for age, sex, resting SBP, and income. Moreover, in hierarchical regression models including the same covariates, carotid IMT continued to covary with extracted amygdala reactivity values when other CVD risk factors (total cholesterol, LDL, and triglycerides) were added to step 1 of the models [left (L) amygdala: $F(1,27) = 8.0$, $\Delta R^2 = 10\%$, $p = .009$; right (R) amygdala: $F(1,27) = 6.7$, $\Delta R^2 = 9\%$, $p = .02$].

In contrast to the dorsal amygdala reactivity findings, carotid IMT did not covary with ventral amygdala reactivity, even at a threshold of $p_{\text{uncorrected}} < .001$, $k = 0$. This null finding unlikely resulted from a failure of the facial expression matching task to engage the ventral amygdala, as dorsal and ventral amygdala reactivity was revealed by the faces > shapes contrast in a whole-brain mixed-effects analysis (Supplements 3 and 4).

Whole-Brain Analysis of Carotid IMT and BOLD Reactivity

The facial expression matching task engaged several areas involved in processing facial expressions, including areas along the fusiform, parahippocampal, and occipital gyri, as well as areas in the orbital, medial-prefrontal, and parietal cortices (Supplements 3 and 4). To explore whether carotid IMT covaried with activation in these areas, we used the whole-brain faces > shapes parametric map as an inclusive mask for a multiple regression analysis of carotid IMT (map illustrated in Supplement 3). Here, carotid IMT did not covary with activation in areas outside the dorsal amygdala, even at a threshold of $p_{\text{uncorrected}} < .001$, $k = 0$.

Carotid IMT and Amygdala-ACC Connectivity

As shown in Figure 3, carotid IMT covaried with a more positive functional connectivity between the right dorsal amygdala and the perigenual area of the rostral ACC, referred to hereafter as pACC (29). As for the dorsal amygdala reactivity findings, this finding was obtained with covariate control for age, sex, resting SBP, and income. Further, in hierarchical regression models with the same covariates, carotid IMT continued to covary with extracted right dorsal amygdala-pACC connectivity values when other CVD risk factors (total cholesterol, LDL, and triglycerides) were added to step 1 of the models [R amygdala-L pACC: $F(1,27) = 27.1$, $\Delta R^2 = 22\%$, $p < .001$; R amygdala-R pACC: $F(1,27) = 25.7$, $\Delta R^2 = 21\%$, $p < .001$].

001]. Covariation between carotid IMT and left amygdala connectivity within the ACC was not observed, even at a threshold of $p_{\text{uncorrected}} < .001, k = 0$.

Whole-Brain Analysis of Carotid IMT and Amygdala Connectivity

In a whole-brain regression analysis, we confirmed that carotid IMT covaried with a more positive functional connectivity between the right dorsal amygdala and the same pACC areas reported above (Supplement 5). Here, carotid IMT also covaried with a more positive connectivity between the right dorsal amygdala and an area of the mid cingulate, as well as a striatal area bordering the caudate and putamen (Supplement 5). As in the ACC ROI findings reported above, no covariation between carotid IMT and left amygdala functional connectivity was observed in this whole-brain analysis, possibly reflecting increased sensitivity of the right amygdala to the negative (angry, fearful) facial expressions used herein (50,51).

Discussion

This study provides initial evidence that preclinical atherosclerosis, measured by carotid IMT, covaries with individual differences in the reactivity and functional connectivity of the amygdala. Moreover, carotid IMT covaried uniquely with amygdala reactivity and connectivity after controlling for traditional CVD risk factors. As such, this evidence implicates individual differences in amygdala functionality as a potential neurobiological parameter of atherosclerotic risk.

Amygdala-Mediated Pathways Potentially Underlying Atherosclerotic Risk

Atherosclerosis is an inflammatory disease process that progresses through clinically silent or preclinical stages well before emergent CVD end points. Carotid IMT is an established measure of preclinical atherosclerosis that has been validated against postmortem markers of atherosclerotic disease and positively associated with traditional CVD risk factors (23-26). Further, use of carotid IMT avoids measurement biases inherent to self-reported symptoms (e.g., angina) and physician diagnoses relying on the expression of late-stage CVD end points. Moreover, carotid IMT is associated with incident CVD events in asymptomatic individuals (23,25). In point, a .10 mm increment in carotid IMT across otherwise healthy adults raises the relative risk for myocardial infarction by 10% to 15% (23). In this regard, it is notable that our participants were unaware of their carotid IMT levels and associated CVD risk estimates. This may have precluded a potentially confounding sensitization of the amygdala and related corticolimbic areas involved in processing threatening or otherwise behaviorally salient information (e.g., the angry and fearful facial expressions used here) among those with higher levels of IMT, who are at presumably greater CVD risk.

While covariation between carotid IMT and amygdala reactivity and connectivity may be clinically relevant, it will be important to determine the mechanisms underlying this covariation. Plausibly, individual differences in amygdala functionality may contribute to alterations in peripheral physiology facilitating atherogenesis. As one line of support for this possibility, animal and epidemiologic studies indicate that individual differences in cardiovascular and neuroendocrine responses to behaviorally salient stimuli are associated with markers of atherosclerosis. For example, cynomolgus macaques exhibiting exaggerated cardiovascular reactions to the threat of capture show increased carotid and coronary atherosclerosis on necropsy (52). Also, humans exhibiting exaggerated stressor-evoked cardiovascular reactions are more likely to show increased carotid IMT compared with their less reactive counterparts (9,12). Finally, humans exhibiting a dysregulated diurnal secretion of cortisol show increased preclinical coronary atherosclerosis (53). Suggesting that amygdala functionality is associated with the potentially atherogenic cardiovascular and neuroendocrine processes noted above, recent neuroimaging evidence has linked amygdala reactivity and

connectivity to both stressor-evoked cardiovascular reactivity (17) and diurnal cortisol secretion (21). In synthesis, the present findings and prior work suggest that individual differences in amygdala functionality may confer atherosclerotic risk via centrally mediated physiological alterations.

Amygdala-ACC Interactions Potentially Involved in Atherosclerotic Risk

Previous independent observations in humans of 1) a positive correlation between amygdala-pACC functional connectivity and exaggerated stressor-evoked cardiovascular reactivity (17) and 2) exaggerated stressor-evoked cardiovascular reactivity and an accelerated prospective increase in carotid IMT (11) suggested that individual differences in amygdala-pACC connectivity may directly account for variability in carotid IMT. Consistent with this suggestion, the present study revealed a direct relationship between amygdala-pACC connectivity and carotid IMT. This relationship may reflect interindividual variation in amygdala-pACC signaling patterns underlying behavioral and physiological processes relevant to atherogenesis. Specifically, fear-conditioning and emotion regulation studies suggest that areas of the rostral ACC, including the pACC, integrate ascending drive from the amygdala to support the processing of behaviorally salient stimuli (27,29,54,55). In turn, rostral ACC areas are thought to exert a descending regulation over the amygdala, particularly during states of fear, anxiety, and stress (56-58). Notably, the pACC and other rostral ACC areas are instrumental for regulating autonomic, cardiovascular, and neuroendocrine activity, particularly via reciprocal signaling with the amygdala (27,29,59,60). Hence, if amygdala-pACC signaling modulates physiological responses to behaviorally salient stimuli, then the differential functional coupling between the amygdala and pACC may influence atherosclerotic risk. To elaborate, individuals exhibiting a stronger descending regulation of the amygdala by the pACC may have a greater capacity to downregulate physiological responses adversely affecting the vasculature. Conversely, stronger ascending drive to the pACC from the amygdala may upregulate the expression of such responses. Both signaling patterns would agree with the finding that individuals exhibiting a more negative amygdala-pACC connectivity showed lesser carotid IMT, whereas individuals exhibiting more positive amygdala-pACC connectivity showed greater carotid IMT.

However, our between-person study design (with one cross-sectional carotid IMT measure per person) and our cross-correlational functional connectivity measures cannot distinguish between presumptive ascending or descending amygdala-pACC signaling patterns linked to carotid IMT. Hence, our ongoing work is employing effective connectivity procedures (49) in conjunction with fMRI task paradigms that 1) involve a broader range of facial expressions than angry and fearful expressions, 2) engage emotion-related regulatory behaviors that modulate ascending and descending amygdala-pACC dynamics, and 3) elicit physiological responses (e.g., stressor-evoked blood pressure changes) related to atherosclerotic risk.

Neurobiological Factors Potentially Impacting Amygdala Functionality and Atherosclerotic Risk

The origins of individual differences in amygdala functionality predicting carotid IMT are uncertain. One possibility involves alterations in serotonergic (5-hydroxytryptamine [5-HT]) neuro-transmission. Specifically, carotid IMT has been shown to covary inversely with central 5-HT responsivity to neuropharmacologic challenge (i.e., intravenous infusion of citalopram, a 5-HT re-uptake inhibitor) (61). This suggests that brain systems sensitive to 5-HT may influence atherogenic mechanisms associated with central 5-HT function, including hypertension (62) and the metabolic syndrome (63). Here, it is also mentionable that patients with major depressive disorder who are treated with selective 5-HT reuptake inhibitors show reduced whole-body noradrenalin spillover, reflecting reduced sympathetic outflow to the heart that may modify CVD risk (64). In view of these observations, it is noteworthy that carotid

IMT in the present study covaried with reactivity and connectivity of the amygdala, which 1) receives projections from dorsal raphe and midbrain serotonergic systems (65), 2) expresses high concentrations of 5-HT receptor subtypes (66), and 3) exhibits marked plasticity as a function of experimental (67) and genetically mediated (68) 5-HT modulation. Thus, 5-HT signaling—possibly linked to heritable and epigenetic factors—may affect atherosclerotic risk through its influence on the functionality of the amygdala and networked corticolimbic areas.

Limitations

One study limitation is that we did not evaluate peripheral physiological or psychosocial factors (e.g., chronic life stress) potentially linked to atherosclerotic risk via alterations in amygdala functionality. A second limitation is that our screening procedures yielded a sample with restricted distributions of traditional CVD risk factors. However, our focus was on preclinical atherosclerosis, and our screening procedures were implemented to control for confounding by cardiovascular and psychiatric disorders on carotid IMT and amygdala functionality. A third limitation is that we cannot exclude the possibility that an unmeasured (third) factor may have contributed to spurious covariation between carotid IMT and amygdala functionality, including shared genetic, behavioral, and environmental factors. Finally, it is possible that arterial atherosclerotic changes impacted our hemodynamic indices of reactivity and connectivity, as measured by BOLD fMRI. Specifically, the BOLD signal reflects blood flow and oxygenation changes in areas of neural activity, which may be compromised by altered microvascular morphology (69). Available evidence and findings from this study, however, counter the interpretation that atherosclerotic changes confounded our BOLD reactivity and connectivity indices. First, cerebral perfusion is not associated with carotid stenosis in CVD patients (70) or carotid IMT in community samples (71), consistent with brain blood flow autoregulatory mechanisms in healthy adults. Second, we detected minimal atherosclerotic plaques in this sample ($n = 4$), and results were unchanged when those with plaques were omitted from analyses. Third, whole-brain analyses revealed no associations between carotid IMT and BOLD activation in areas outside the amygdala, suggesting no diffuse BOLD signal alterations across the brain. Our findings, therefore, do not appear to be due to confounding neurovascular factors.

Conclusions

Individuals expressing a thickening of the carotid intima-media vessel wall complex—an indicator of preclinical atherosclerosis—also express heightened amygdala reactivity and a more positive functional connectivity between the amygdala and pACC. The amygdala and its functional interactions with the pACC have long been implicated in conferring risk for psychopathologies of mood and anxiety (72-74). This study further indicates that individual differences in amygdala and related pACC functionality may also confer risk for atherosclerosis and CVD.

Supplementary Material

Refer to Web version on PubMed Central for supplementary material.

Acknowledgments

This work was supported by National Institutes of Health Grants P01 HL40962 and RO1 HL065137 (SBM), K01 MH072837 (ARH), and K01 MH070616 and R01 HL089850 (PJG).

We thank Sarah Abramowitch for assisting in study execution, and Drs. J. Richard Jennings, Ilan Kerman, and Bruce McEwen for commenting on a draft of this manuscript.

References

1. Rosamond W, Flegal K, Furie K, Go A, Greenlund K, Haase N, et al. Heart disease and stroke statistics--2008 update: A report from the American Heart Association Statistics Committee and Stroke Statistics Subcommittee. *Circulation* 2008;117:e25–146. [PubMed: 18086926]
2. Hemingway H, Marmot M. Psychosocial factors in the aetiology and prognosis of coronary heart disease: Systematic review of prospective cohort studies. *BMJ* 1999;318:1460–1467. [PubMed: 10346775]
3. Grippo A, Johnson K. Biological mechanisms in the relationship between depression and heart disease. *Neurosci Biobehav Rev* 2002;26:941–962. [PubMed: 12667498]
4. Carney R, Freedland K. Depression, mortality, and medical morbidity in patients with coronary heart disease. *Biol Psychiatry* 2003;54:241–247. [PubMed: 12893100]
5. Rudisch B, Nemeroff C. Epidemiology of comorbid coronary artery disease and depression. *Biol Psychiatry* 2003;54:227–240. [PubMed: 12893099]
6. Libby P. Inflammation in atherosclerosis. *Nature* 2002;420:868–874. [PubMed: 12490960]
7. Revkin JH, Shear CL, Pouleur HG, Ryder SW, Orloff DG. Biomarkers in the prevention and treatment of atherosclerosis: Need, validation, and future. *Pharmacol Rev* 2007;59:40–53. [PubMed: 17329547]
8. Brotman DJ, Golden SH, Wittstein IS. The cardiovascular toll of stress. *Lancet* 2007;370:1089–1100. [PubMed: 17822755]
9. Gianaros PJ, Bleil ME, Muldoon MF, Jennings JR, Sutton-Tyrrell K, McCaffery JM, et al. Is cardiovascular reactivity associated with atherosclerosis among hypertensives? *Hypertension* 2002;40:742–747. [PubMed: 12411471]
10. Kamarck T, Everson S, Kaplan G, Manuck S, Jennings J, Salonen R, et al. Exaggerated blood pressure responses during mental stress are associated with enhanced carotid atherosclerosis in middle aged Finnish men: Findings from the Kuopio Ischemic Heart Disease Study. *Circulation* 1997;96:3842–3848. [PubMed: 9403606]
11. Jennings J, Kamarck T, Everson-Rose S, Kaplan G, Manuck S, Salonen J. Exaggerated blood pressure responses during mental stress are prospectively related to enhanced carotid atherosclerosis in middle-aged Finnish men. *Circulation* 2004;110:2198–2203. [PubMed: 15451789]
12. Treiber FA, Kamarck T, Schneiderman N, Sheffield D, Kapuku G, Taylor T. Cardiovascular reactivity and development of preclinical and clinical disease states. *Psychosom Med* 2003;65:46–62. [PubMed: 12554815]
13. Kaplan J, Pettersson K, Manuck S, Olsson G. Role of sympathoadrenal medullary activation in the initiation and progression of atherosclerosis. *Circulation* 1991;84(6 suppl):V123–132.
14. Manuck SB, Kaplan JR, Adams MR, Clarkson TB. Effects of stress and the sympathetic nervous system on coronary artery atherosclerosis in the cynomolgus macaque. *Am Heart J* 1988;116:328–333. [PubMed: 2899392]
15. Manuck SB, Kaplan JR, Clarkson TB. Behaviorally induced heart rate reactivity and atherosclerosis in cynomolgus monkeys. *Psychosom Med* 1983;45:95–108. [PubMed: 6683414]
16. McEwen BS. Physiology and neurobiology of stress and adaptation: Central role of the brain. *Physiol Rev* 2007;87:873–904. [PubMed: 17615391]
17. Gianaros PJ, Sheu LK, Matthews KA, Jennings JR, Manuck SB, Hariri AR. Individual differences in stressor-evoked blood pressure reactivity vary with activation, volume, and functional connectivity of the amygdala. *J Neurosci* 2008;28:990–999. [PubMed: 18216206]
18. Amaral DG, Price JL. Amygdalo-cortical projections in the monkey (*Macaca fascicularis*). *J Comp Neurol* 1984;230:465–496. [PubMed: 6520247]
19. Dampney RA. Functional organization of central pathways regulating the cardiovascular system. *Physiol Rev* 1994;74:323–364. [PubMed: 8171117]
20. Neumann SA, Brown SM, Ferrell RE, Flory JD, Manuck SB, Hariri AR. Human choline transporter gene variation is associated with corticolimbic reactivity and autonomic-cholinergic function. *Biol Psychiatry* 2006;60:1155–1162. [PubMed: 16876130]
21. Urry HL, van Reekum CM, Johnstone T, Kalin NH, Thurow ME, Schaefer HS, et al. Amygdala and ventromedial prefrontal cortex are inversely coupled during regulation of negative affect and predict

- the diurnal pattern of cortisol secretion among older adults. *J Neurosci* 2006;26:4415–4425. [PubMed: 16624961]
22. Furberg CD, Adams HP Jr, Applegate WB, Byington RP, Espeland MA, Hartwell T, et al. Asymptomatic Carotid Artery Progression Study (ACAPS) Research Group. Effect of lovastatin on early carotid atherosclerosis and cardiovascular events. *Circulation* 1994;90:1679–1687. [PubMed: 7734010]
 23. Lorenz MW, Markus HS, Bots ML, Rosvall M, Sitzer M. Prediction of clinical cardiovascular events with carotid intima-media thickness: A systematic review and meta-analysis. *Circulation* 2007;115:459–467. [PubMed: 17242284]
 24. Blankenhorn DH, Selzer RH, Crawford DW, Barth JD, Liu CR, Liu CH, et al. Beneficial effects of colestipol-niacin therapy on the common carotid artery: Two- and four-year reduction of intima-media thickness measured by ultrasound. *Circulation* 1993;88:20–28. [PubMed: 8319334]
 25. Craven TE, Ryu JE, Espeland MA, Kahl FR, McKinney WM, Toole JF, et al. A case-control study. Evaluation of the associations between carotid artery atherosclerosis and coronary artery stenosis. *Circulation* 1990;82:1230–1242. [PubMed: 2205416]
 26. Probstfield JL, Byington RP, Egan DA, Espeland MA, Margitic SE, Riley WA Jr, et al. Methodological issues facing studies of atherosclerotic change. *Circulation* 1993;87(3 suppl):II74–81. [PubMed: 8443927]
 27. Critchley HD. Neural mechanisms of autonomic, affective, and cognitive integration. *J Comp Neurol* 2005;493:154–166. [PubMed: 16254997]
 28. Pezawas L, Meyer-Lindenberg A, Drabant EM, Verchinski BA, Munoz KE, Kolachana BS, et al. 5-HTTLPR polymorphism impacts human cingulate-amygdala interactions: A genetic susceptibility mechanism for depression. *Nat Neurosci* 2005;8:828–834. [PubMed: 15880108]
 29. Vogt BA. Pain and emotion interactions in subregions of the cingulate gyrus. *Nat Rev Neurosci* 2005;6:533–544. [PubMed: 15995724]
 30. Brown SM, Manuck SB, Flory JD, Hariri AR. Neural basis of individual differences in impulsivity: Contributions of corticolimbic circuits for behavioral arousal and control. *Emotion* 2006;6:239–245. [PubMed: 16768556]
 31. First, MB.; Spitzer, RL.; Gibbon, M.; Williams, JBW. Structured Clinical Interview for DSM-IV Axis I Disorders, Research Version, Non-Patient Edition. New York State Psychiatric Institute, Biometrics Research Department; New York: 1996.
 32. Muldoon MF, Nazzaro P, Sutton-Tyrrell K, Manuck SB. White-coat hypertension and carotid artery atherosclerosis: A matching study. *Arch Intern Med* 2000;160:1507–1512. [PubMed: 10826466]
 33. Matthews KA. Psychological perspectives on the development of coronary heart disease. *Am Psychol* 2005;60:783–796. [PubMed: 16351405]
 34. Radloff LS. The CES-D scale: A self-report depression scale for research in the general population. *Appl Psychol Meas* 1977;1:385–401.
 35. Spielberger, C.; Gorsuch, R.; Lushene, R. STAI Manual for the State-Trait Anxiety Inventory. Consulting Psychologists Press Inc.; Palo Alto, CA: 1970.
 36. Sutton-Tyrrell K, Wolfson SK Jr, Thompson T, Kelsey SF. Measurement variability in duplex scan assessment of carotid atherosclerosis. *Stroke* 1992;23:215–220. [PubMed: 1561650]
 37. Thompson T, Sutton-Tyrrell K, Wildman R. Continuous quality assessment programs can improve carotid duplex scan quality. *J Vasc Tech* 2001;25:33–39.
 38. Wendelhag I, Liang Q, Gustavsson T, Wikstrand J. A new automated computerized analyzing system simplifies readings and reduces the variability in ultrasound measurement of intima-media thickness. *Stroke* 1997;28:2195–2200. [PubMed: 9368564]
 39. Manuck SB, Brown SM, Forbes EE, Hariri AR. Temporal stability of individual differences in amygdala reactivity. *Am J Psychiatry* 2007;164:1613–1614. [PubMed: 17898358]
 40. Hariri AR, Mattay VS, Tessitore A, Fera F, Smith WG, Weinberger DR. Dextroamphetamine modulates the response of the human amygdala. *Neuropsychopharmacology* 2002;27:1036–1040. [PubMed: 12464460]
 41. Hariri AR, Mattay VS, Tessitore A, Kolachana B, Fera F, Goldman D, et al. Serotonin transporter genetic variation and the response of the human amygdala. *Science* 2002;297:400–403. [PubMed: 12130784]

42. Ekman, P.; Friesen, WV. Pictures of Facial Affect. Consulting Psychologists Press; Palo Alto, CA: 1976.
43. Davis M, Whalen PJ. The amygdala: Vigilance and emotion. *Mol Psychiatry* 2001;6:13–34. [PubMed: 11244481]
44. LeDoux JE. Emotion circuits in the brain. *Annu Rev Neurosci* 2000;23:155–184. [PubMed: 10845062]
45. Sah P, Faber ES, Lopez De Armentia M, Power J. The amygdaloid complex: Anatomy and physiology. *Physiol Rev* 2003;83:803–834. [PubMed: 12843409]
46. Zald DH. The human amygdala and the emotional evaluation of sensory stimuli. *Brain Res Brain Res Rev* 2003;41:88–123. [PubMed: 12505650]
47. Genovese CR, Lazar NA, Nichols T. Thresholding of statistical maps in functional neuroimaging using the false discovery rate. *Neuroimage* 2002;15:870–878. [PubMed: 11906227]
48. Brett, M.; Anton, J.; Valabregue, R.; Poline, J. Region of interest analysis using an SPM toolbox [abstract on CD-ROM]; Presented at the 8th International Conference on Functional Mapping of the Human Brain; Sendai, Japan. June 2–6, 2002; 2002. *Neuroimage* 16
49. Friston K. Functional and effective connectivity in neuroimaging: A synthesis. *Hum Brain Mapp* 1994;2:56–78.
50. Baas D, Aleman A, Kahn RS. Lateralization of amygdala activation: A systematic review of functional neuroimaging studies. *Brain Res Brain Res Rev* 2004;45:96–103. [PubMed: 15145620]
51. Noesselt T, Driver J, Heinze HJ, Dolan R. Asymmetrical activation in the human brain during processing of fearful faces. *Curr Biol* 2005;15:424–429. [PubMed: 15753036]
52. Manuck SB, Marsland AL, Kaplan JR, Williams JK. The pathogenicity of behavior and its neuroendocrine mediation: An example from coronary artery disease. *Psychosom Med* 1995;57:275–283. [PubMed: 7652128]
53. Matthews K, Schwartz J, Cohen S, Seeman T. Diurnal cortisol decline is related to coronary calcification: CARDIA study. *Psychosom Med* 2006;68:657–661. [PubMed: 17012518]
54. Bush G, Luu P, Posner MI. Cognitive and emotional influences in anterior cingulate cortex. *Trends Cogn Sci* 2000;4:215–222. [PubMed: 10827444]
55. Phillips ML, Drevets WC, Rauch SL, Lane R. Neurobiology of emotion perception I: The neural basis of normal emotion perception. *Biol Psychiatry* 2003;54:504–514. [PubMed: 12946879]
56. Etkin A, Egner T, Peraza DM, Kandel ER, Hirsch J. Resolving emotional conflict: A role for the rostral anterior cingulate cortex in modulating activity in the amygdala. *Neuron* 2006;51:871–882. [PubMed: 16982430]
57. Ochsner KN, Gross JJ. The cognitive control of emotion. *Trends Cogn Sci* 2005;9:242–249. [PubMed: 15866151]
58. Quirk GJ, Beer JS. Prefrontal involvement in the regulation of emotion: Convergence of rat and human studies. *Curr Opin Neurobiol* 2006;16:723–727. [PubMed: 17084617]
59. Öngür D, Ferry AT, Price JL. Architectonic subdivision of the human orbital and medial prefrontal cortex. *J Comp Neurol* 2003;460:425–449. [PubMed: 12692859]
60. Price JL. Comparative aspects of amygdala connectivity. *Ann N Y Acad Sci* 2003;985:50–58. [PubMed: 12724147]
61. Muldoon MF, Mackey RH, Sutton-Tyrrell K, Flory JD, Pollock BG, Manuck SB. Lower central serotonergic responsivity is associated with preclinical carotid artery atherosclerosis. *Stroke* 2007;38:2228–2233. [PubMed: 17626900]
62. Stocker SD, Muldoon MF, Sved AF. Blunted fenfluramine-evoked prolactin secretion in hypertensive rats. *Hypertension* 2003;42:719–724. [PubMed: 12885788]
63. Muldoon MF, Mackey RH, Korytkowski MT, Flory JD, Pollock BG, Manuck SB. The metabolic syndrome is associated with reduced central serotonergic responsivity in healthy community volunteers. *J Clin Endocrinol Metab* 2006;91:718–721. [PubMed: 16303834]
64. Barton DA, Dawood T, Lambert EA, Esler MD, Haikerwal D, Brenchley C, et al. Sympathetic activity in major depressive disorder: Identifying those at increased cardiac risk? *J Hypertens* 2007;25:2117–2124. [PubMed: 17885556]

65. Sadikot AF, Parent A. The monoaminergic innervation of the amygdala in the squirrel monkey: An immunohistochemical study. *Neuroscience* 1990;36:431–447. [PubMed: 1977101]
66. Varnas K, Halldin C, Hall H. Autoradiographic distribution of serotonin transporters and receptor subtypes in human brain. *Hum Brain Mapp* 2004;22:246–260. [PubMed: 15195291]
67. Cools R, Calder AJ, Lawrence AD, Clark L, Bullmore E, Robbins TW. Individual differences in threat sensitivity predict serotonergic modulation of amygdala response to fearful faces. *Psychopharmacology (Berl)* 2005;180:670–679. [PubMed: 15772862]
68. Canli T, Lesch K-P. Long story short: The serotonin transporter in emotion regulation and social cognition. *Nat Neurosci* 2007;10:1103–1109. [PubMed: 17726476]
69. Logothetis NK. The neural basis of the blood-oxygen-level-dependent functional magnetic resonance imaging signal. *Philos Trans R Soc Lond B Biol Sci* 2002;357:1003–1037. [PubMed: 12217171]
70. van Laar PJ, van der Graaf Y, Mali WP, van der Grond J, Hendrikse J. Effect of cerebrovascular risk factors on regional cerebral blood flow. *Radiology* 2008;246:198–204. [PubMed: 18033756]
71. Claus JJ, Breteler MM, Hasan D, Krenning EP, Bots ML, Grobbee DE, et al. Vascular risk factors, atherosclerosis, cerebral white matter lesions and cerebral perfusion in a population-based study. *Eur J Nucl Med* 1996;23:675–682. [PubMed: 8662102]
72. Drevets WC. Functional anatomical abnormalities in limbic and prefrontal cortical structures in major depression. *Prog Brain Res* 2000;126:413–431. [PubMed: 11105660]
73. Mayberg HS. Modulating dysfunctional limbic-cortical circuits in depression: Towards development of brain-based algorithms for diagnosis and optimised treatment. *Br Med Bull* 2003;65:193–207. [PubMed: 12697626]
74. Phillips ML, Drevets WC, Rauch SL, Lane R. Neurobiology of emotion perception II: Implications for major psychiatric disorders. *Biol Psychiatry* 2003;54:515–528. [PubMed: 12946880]

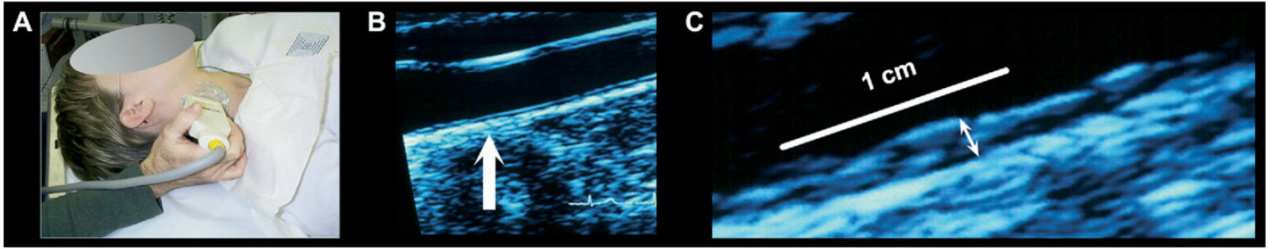


Figure 1.

Carotid intima-media thickness (IMT) was assessed by B-mode ultrasonography. (A) A vascular technologist imaged the carotid arteries for later automated scoring of IMT. (B) An image of the carotid artery with the common carotid segment visible at right and the beginning of the carotid bulb visible at left. The arrow indicates a point along the far wall of the common carotid artery, which is shown at higher magnification in (C). (C) Magnified point of the far wall of the common carotid artery illustrating the lumen-intima and media-adventitia interfaces. IMT was measured by averaging the intima-media thickness (the distance between two lines tracking the lumen-intima and media-adventitia interfaces, not illustrated here) in 1 mm increments along the distal 1 cm of the far wall of the common carotid artery, the far wall of the carotid bulb, and the first cm of the internal carotid artery.

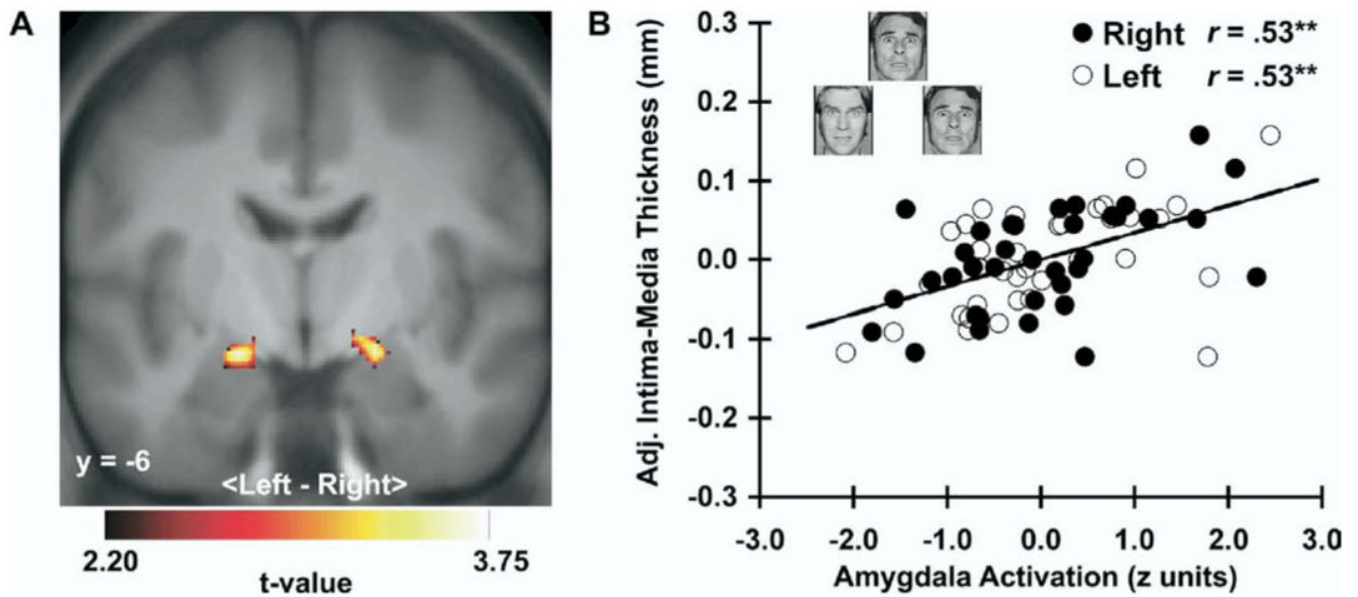


Figure 2.

Carotid intima-media thickness (IMT) covaried positively with dorsal amygdala reactivity to angry and fearful facial expressions. **(A)** Parametric maps from an ROI regression analysis identifying clusters of the left [MNI coordinates: $-16, -8, -14$; $t(30) = 3.72, z = 3.34, p_{\text{FDR}} = .02, p_{\text{uncorrected}} < .001, k = 87$] and right [$20, -6, -14$; $t(30) = 3.56, z = 3.23, p_{\text{FDR}} = .03, p_{\text{uncorrected}} = .001, k = 63$] areas of the dorsal amygdala where carotid IMT covaried with amygdala reactivity after covariate control for age, sex, resting systolic blood pressure, and family income. Maps are masked by an anatomical amygdala ROI, are shown at an ROI-volume corrected threshold ($p_{\text{FDR}} < .05, k = 20$), and are projected onto a coronal section of an averaged MNI-transformed template derived from study participants. **(B)** Covariate-adjusted IMT is shown as a function of mean-centered and standardized amygdala BOLD activation values (faces > shapes contrast parameters, see Methods and Materials) extracted from the peak voxels of the left (L, open circles, dashed line) and right (R, closed circles, solid line) amygdala clusters profiled in **(A)**. Inset in **(B)** illustrates sample trial from the facial expression matching task designed to elicit amygdala reactivity. $**p < .001$. BOLD, blood oxygenation level-dependent; L, left; MNI, Montreal Neurological Institute; R, right; ROI, region of interest. Face stimuli copyrighted by Paul Ekman (Ekman and Friesen [1976], reprinted with permission).

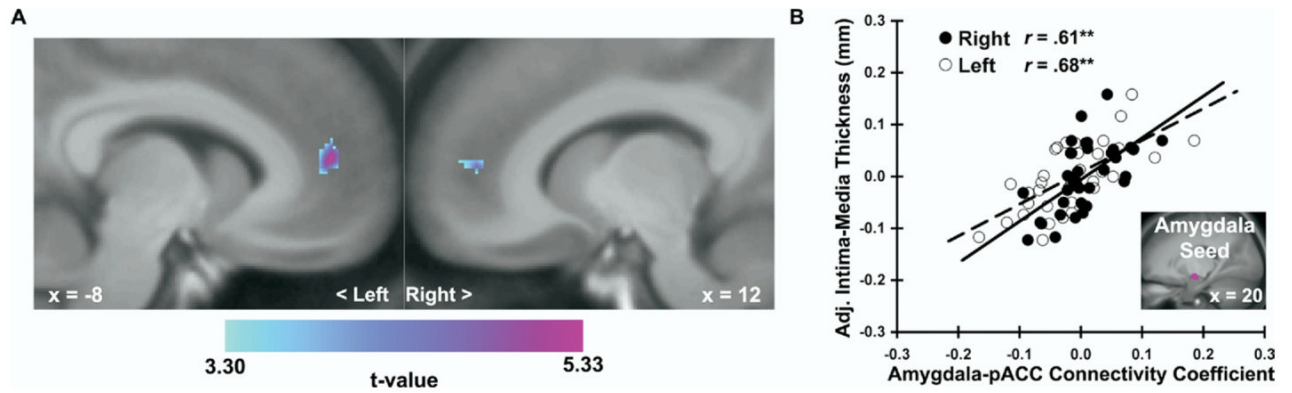


Figure 3.

Carotid intima-media thickness (IMT) covaried with a more positive functional connectivity between the right dorsal amygdala and perigenual area of the rostral anterior cingulate cortex (pACC). **(A)** Parametric maps from an ROI regression analysis illustrating areas of the pACC where carotid IMT varied across individuals as a function of connectivity with a right amygdala seed (5 mm sphere surrounding MNI coordinates: 20, -6, -14), after covariate control for age, sex, resting systolic blood pressure, and family income. Maps are masked by an anatomical ACC ROI, are shown at an ROI-volume corrected threshold ($p_{\text{FDR}} < .05$, $k = 20$), and are projected onto sagittal sections of an averaged MNI-transformed template derived from study participants. Left pACC coordinates: -8, 50, 12; $t(30) = 5.33$, $z = 4.44$, $p_{\text{FDR}} = .01$, $p_{\text{uncorrected}} < .001$, $k = 104$; right pACC: 12, 50, 8; $t(30) = 4.56$, $z = 3.94$, $p_{\text{FDR}} = .01$, $p_{\text{uncorrected}} < .001$, $k = 44$. **(B)** Covariate-adjusted carotid IMT is shown as a function of connectivity coefficients extracted for each individual from the peak voxels of the left (L, open circles, dashed line) and right (R, closed circles, solid line) pACC clusters profiled in **(A)**. Inset in **(B)** shows amygdala seed region used for connectivity analyses. $**p < .001$. ACC, anterior cingulate cortex; L, left; MNI, Montreal Neurological Institute; pACC, perigenual area of the rostral anterior cingulate cortex; R, right; ROI, region of interest.

Table 1

Sample Characteristics and Univariate Correlations Between Cardiovascular Risk Factors and Carotid IMT in 18 Men and 18 Women

Variable	Descriptive Statistics		Correlation with IMT
	M or <i>n</i>	SD	<i>r</i>
Demographic Variables			
Age (years)	44.3	6.8	.52 ^b
Education (years)	16.4	2.7	.12
Annual income (U.S. \$)			.37 ^a
< 49,999K	11		
50,000 – 80,000K	15		
> 80,000K	10		
Psychological Variables			
Depressive symptoms (CES-D)	4.3	4.3	-.05
Dispositional anxiety (STAI-T)	29.9	8.9	-.10
Cardiovascular Risk Factors			
BMI (kg/m ²)	26.7	4.4	.06
SBP (mmHg)	112.9	11.6	.33 ^a
DBP (mmHg)	76.1	7.6	.32
Total cholesterol (mmol/L)	11.3	2.0	.27
HDL (mmol/L)	3.3	.9	.04
Triglycerides (mmol/L)	6.3	3.0	.21
LDL (mmol/L)	6.8	1.7	.22
Fasting glucose (mmol/L)	5.2	.4	.11
Fasting insulin (μU/mL)	13.2	7.1	-.04
Mean carotid IMT (mm)	.66	.09	—

Note: White, *n* = 33 (91.7%), current smokers, *n* = 1 (2.8%).

Participants' income in U.S. dollars is presented in three categories but was coded according to eight categories (< \$10K; \$10–14,999K; \$15–24,999K; \$25–34,999K; \$35–49,999K; \$50–64,999K; \$65–79,999K; and ≥ \$80K). Mean carotid IMT differed significantly between men (*M* = .70, *SD* = .11 mm) and women (*M* = .63, *SD* = .05 mm), *t*(34) = 2.65, *p* = .01.

BMI, body mass index; CES-D, Center for Epidemiologic Studies Depression Scale (past week); DBP, diastolic blood pressure; HDL, high-density lipoproteins; IMT, intima-media thickness; LDL, low-density lipoproteins; SBP, systolic blood pressure; STAI-T, State-Trait Anxiety Inventory (Trait Version).

^a *p* < .05.

^b *p* < .01.